Automatica 194 (2026) 113261

Contents lists available at ScienceDirect

Automatica

journal homepage: www.elsevier.com/locate/automatica

Brief paper

Delay injection-based fixed-time interval state estimation for perturbed linear systems ☆

Longwen Liu [a,*], Thach Ngoc Dinh [b]

[a] School of Automation and Electronic Information, Xiangtan University, Xiangtan, Hunan, 411105, China
[b] Conservatoire National des Arts et Métiers, Cedric-Lab, 292 rue St-Martin, Paris Cedex 03, 75141, France

ARTICLE INFO

Article history:
Received 21 August 2025
Received in revised form 29 March 2026
Accepted 18 July 2026

Keywords:
Interval estimation
Perturbed systems
Fixed-time convergence
Parametric method

ABSTRACT

This paper investigates fixed-time interval state estimation (F-ISE) methods for perturbed continuous- and discrete-time linear systems. A novel delay injection-based non-smooth F-ISE structure is proposed, using computed bounds on the piecewise observation error. The existence conditions of this F-ISE structure are formulated as constrained matrix equations (MEs) that impose no additional requirements on the system matrix, fixed-time constant, or measurement noise. By solving these MEs, a parametric feasible solution for the F-ISE is obtained under a common observability condition, providing explicit design degrees of freedom for further component-wise optimization. Additionally, we present a detailed discussion on the relationship between the proposed method and the extensions of this non-smooth structure in comparison with other existing ISE methods. Finally, two comparative simulations demonstrate the advantages of the proposed approach over existing methods.

1. Introduction

State estimation is a crucial technique for many control tasks (Kalman, 1960; Luenberger, 1971), especially when measuring all states is impractical due to cost constraints, limited sensor availability, or environmental challenges. System uncertainties impose significant demands on state estimation across various applications. Interval state estimation (ISE), which seeks to determine guaranteed state intervals at each time instant, is an alternative approach that reduces estimation complexity for a broad class of perturbed systems. This method has gained substantial attention as a research topic over recent decades.

In early research (Alamo et al., 2005; Chisci et al., 1996; Schweppe, 1968), ISE was achieved through an intersection-based correction between the state prediction set and the measurement update set, relying on uncertainty propagation in the system's state equations. However, this approach incurs high computational costs, and the set representations are not always closed under correction (Althoff & Rath, 2021). To address these issues, a Luenberger-like observer was introduced as the new propagation carrier of system uncertainties, enhancing computational efficiency and allowing more design flexibility. This framework has become widely used in set-propagation-based ISEs (SP-ISEs) (Huang et al., 2021; Tang et al., 2019; Wang et al., 2024; Wang, Zhang et al., 2022c; Zhou et al., 2025), although it primarily applies to discrete-time (DT) systems. Gouzé et al. (2000) proposed an ISE approach for continuous-time (CT) and DT systems using a monotone system-based interval observer (IO). This approach constructs state intervals via a pair of auxiliary dynamic systems in a Luenberger-like structure, possessing higher computational efficiency than SP-ISEs (Xu, 2021) and proving valuable in ISE applications (Efimov & Raïssi, 2016; Ethabet et al., 2018; Zhu & Li, 2024). Despite this, IO-based ISEs face greater design and estimation conservatism compared to SP-ISEs due to monotonicity constraints and simple bounding structures (Efimov & Raïssi, 2016; Tang et al., 2019). Xu, Yang, and Liang (2020b) introduced a hybrid approach that balances computational efficiency and estimation conservatism by combining IO and SP-ISE methods.

In many applications, fast convergence of state estimation is essential for timely fault detection and accurate control, particularly during early equipment operation. Many studies have incorporated finite- or fixed-time stability into observer design to address these needs (Engel & Kreisselmeier, 2002; Lopez-Ramirez et al., 2018; Mazenc et al., 2022; Zhang et al., 2025). However, relatively little research has been devoted to ISE (Dinh et al., 2019, 2020; Huang et al., 2018; Khan et al., 2021, 2020; Liu et al., 2020; Ma et al., 2019; Meslem & Ramdani, 2020; Sun et al., 2020; Wang, Dinh et al., 2022a), and only two works (Liu et al., 2020; Ma

☆ This work was supported by the Scientific Research Starting Foundation of Xiangtan University, the Scientific Research Fund of Hunan Provincial Education Department (25C0068, 25B0168), the Provincial Natural Science Foundation of Hunan (2025JJ50391). The material in this paper was not presented at any conference. This paper was recommended for publication in revised form by Associate Editor Laurentiu Hetel under the direction of Editor Maria Elena Valcher.

* Corresponding author.
E-mail addresses: lw_liu@xtu.edu.cn (L. Liu), ngoc-thach.dinh@lecnam.net (T.N. Dinh).

https://doi.org/10.1016/j.automatica.2026.113261

et al., 2019) focus on CT systems. These approaches can be divided into three categories: (1) Gain and switching signal design via multiple linear copositive Lyapunov functions and average dwell time, which applies only to switched systems and is constrained by the switching signal (Huang et al., 2018; Ma et al., 2019; Sun et al., 2020); (2) Non-smooth IO dynamics leveraging delay properties (Dinh et al., 2019, 2020; Liu et al., 2020); however, the works of Dinh et al. require an invertible system matrix, while Liu et al.'s approach increases conservatism due to noise derivatives (Liu et al., 2020); and (3) A backward propagation approach using output sequences over a time window, limited to DT systems with convergence constraints based on system dimensions (Khan et al., 2021, 2020; Meslem & Ramdani, 2020; Wang, Dinh et al., 2022a).

To address these gaps, we propose a unified fixed-time ISE (F-ISE) for CT and DT linear time-invariant (LTI) systems, combining a non-smooth observer structure and bounded error computation. The main contributions are as follows:

- A less conservative delay-injection-based non-smooth F-ISE structure to address existing limitations.
- A parametric design method for the F-ISE with an optimization index, showcasing available design flexibility.
- A theoretical comparison of estimation conservatism between the proposed method and other IO-ISE and SP-ISE-based approaches.

The paper is structured as follows: Section 2 covers preliminaries and the problem statement. Main results and comparative analyses are presented in Sections 3 and 4. Section 5 provides simulation comparisons to illustrate the advantages of the proposed method.

2. Preliminaries and problem statement

The notations are defined as follows: $\mathbb{R}^{n\times m}$ and $\mathbb{C}^{n\times m}$ respectively denote the sets of real and complex matrices with $n \times m$ dimensions. I_n and 0 represent the identity matrix of dimension n and the zero matrix of appropriate dimensions. Relations for vectors or matrices, such as $p_1 \leq p_2$ or $M_1 > M_2$, as well as their absolute values $|p|$ or $|M|$, are understood element-wise, which implies $|p_1 + p_2| \leq |p_1| + |p_2|$ and $|Mp| \leq |M|\,|p|$. The notation $\mathbf{exp}[Mt]$ denotes the exponential function of Mt with the natural constant e as the base. $\mathbf{max}\big[A, B\big]$ returns the element-wise maximum values between matrices A and B, and $A^{\mathrm{u}} = \mathbf{max}\big[A, 0\big]$, $A^{\mathrm{d}} = A^{\mathrm{u}} - A$. Given a column vector $d \in \mathbb{R}^n$, $\mathbf{diag}\big[d\big]$ denotes the diagonal matrix whose diagonal entries are $d_1, d_2, \ldots, d_n$. $\odot$ represents a linear mapping, $\oplus$ is the Minkowski sum, and $\bigoplus$ denote the Minkowski sum of a series of sets.

Definition 1 (*Huang et al., 2021*)**.** An m-order zonotope in the n-dimensional space is defined as $\mathbf{Z} = \langle p, H\rangle = \big\{\, p + Hz : z \in \mathbb{B}^m \,\big\}$, where $p \in \mathbb{R}^n$ is the center of $\mathbf{Z}$, $H \in \mathbb{R}^{n\times m}$ is the shape matrix of $\mathbf{Z}$, and $\mathbb{B}^m = [-1, 1]^m$ is a hypercube.

Given the matrices $p_1, p_2 \in \mathbb{R}^n$, $H_1, H_2 \in \mathbb{R}^{n\times m}$ and $L \in \mathbb{R}^{l\times n}$, there are $\big\langle p_1, H_1\big\rangle \oplus \big\langle p_2, H_2\big\rangle = \big\langle p_1 + p_2, H_1 + H_2\big\rangle$ and $L \odot \big\langle p_1, H_1\big\rangle = \big\langle Lp_1, LH_1\big\rangle$.

Definition 2. Any square matrix is called: (a) Metzler if all its non-diagonal elements are non-negative; (b) Hurwitz if the real parts of all its eigenvalues are negative; (c) Schur if all its eigenvalues lie within the unit circle; (d) Nonnegative if all its elements are non-negative.

In this paper, the term **stable matrix** refers to a Hurwitz matrix in the CT case and a Schur matrix in the DT case. Likewise, the term **monotone matrix** refers to a Metzler matrix in the CT case and a nonnegative matrix in the DT case.

Definition 3. A fixed-time observer for the uncertain system $x(t)$ at a pre-defined step t_d is a reconstructed state $\hat{x}(t)$ such that the error $e(t) = \hat{x}(t) - x(t)$ is bounded for all times and exactly converges to zero when uncertainties are ignored and $t \geq t_d$.

Definition 4 (*Duan, 2015*)**.** Given $A \in \mathbb{R}^{n\times n}$, $B \in \mathbb{R}^{n\times m}$, a pair of polynomial matrices $X(s)$ and $Y(s)$ is called a pair of right coprime polynomial matrices associated with the pair (A, B), if $\big(sI_n - A\big)X(s) - BY(s) = 0$ and $X(s)$, $Y(s)$ satisfy the Bézout identity.

As pointed out in Duan (2015), if the pair (A, B) is controllable, then a pair of right coprime polynomial matrices $X(s)$ and $Y(s)$ exists.

Lemma 5 (*Huang et al., 2021*)**.** *For an m-order zonotope* $\mathbf{Z} = \big\langle p, H\big\rangle$ *in the n-dimensional space, the operation* $[\underline{z}, \overline{z}] = \mathbf{Hull}\,[Z]$ *is denoted as*

$$\begin{cases} \underline{z}_i = p_i - \displaystyle\sum_{j=1}^{m} \big|H_{i,j}\big|, \; i = 1, 2, \ldots, n, \\ \overline{z}_i = p_i + \displaystyle\sum_{j=1}^{m} \big|H_{i,j}\big|, \; i = 1, 2, \ldots, n, \end{cases}$$

Lemma 6. *Consider an integral function vector* $F(t, t_0) = \int_{t_0}^{t} \mathbf{exp}\big[\Phi(t-\tau)\big]\Psi u(\tau)\mathbf{d}\tau$*, where* t_0 *is a scalar constant,* $\Phi \in \mathbb{R}^{n\times n}$*,* $\Psi \in \mathbb{R}^{n\times m}$*, and* $|u(t)| \leq U \in \mathbb{R}^m$*. Then, a componentwise bound for* $F(t, t_0)$ *is* $|F(t, t_0)| \leq \gamma(t)$*, where* $\gamma(t)$ *satisfies* $\dot{\gamma}(t) = \big|\mathbf{exp}\big[\Phi(t - t_0)\big]\Psi\big|\,U$ *with* $\gamma(t_0) = 0$*. Moreover, if* Φ *is nonsingular and Metzler, there exists* $\gamma_M(t) = \frac{1}{\Phi}\big(\mathbf{exp}\big[\Phi(t-t_0)\big] - I_n\big)\,|\Psi|\,U$ *such that* $\gamma(t) \leq \gamma_M(t)$*.*

Proof. For $F(t, t_0)$, we have $|F(t, t_0)| = \Big|\int_{t_0}^{t} \mathbf{exp}\big[\Phi(t-\tau)\big]\Psi u(\tau)\,\mathbf{d}\tau\Big| \leq \int_{t_0}^{t} \big|\mathbf{exp}\big[\Phi(t-\tau)\big]\Psi\big|\,\mathbf{d}\tau U = \gamma(t)$, based on (Meslem et al., 2020), implying $|F(t, t_0)| \leq \gamma(t)$. Next, choose a scalar $\mu \geq \mathbf{max}_{1\leq i\leq n}\left[-\Phi_{ii}, 0\right]$, and given the Metzler matrix Φ, we can always obtain a Nonnegative matrix $\Phi_M = \Phi + \mu I_n$. Let $s = t - \tau$, and when $t_0 \leq \tau \leq t$, there is $\mathbf{exp}\big[\Phi(t-\tau)\big] = \mathbf{exp}\big[\Phi s\big] = \mathbf{exp}\big[(\Phi_M - \mu I_n)s\big] = \mathbf{exp}\big[-\mu s\big]\mathbf{exp}\big[\Phi_M s\big] = \mathbf{exp}\big[-\mu s\big]\sum_{k=0}^{\infty}\frac{s^k}{k!}\Phi_M^k \geq 0$. Then, according to the above deduced condition and nonsingular matrix Φ, we have

$$\begin{aligned} \gamma(t) &= \int_{t_0}^{t} \big|\mathbf{exp}\big[\Phi(t-\tau)\big]\Psi\big|\,\mathbf{d}\tau U \\ &\leq \int_{t_0}^{t} \big|\mathbf{exp}\big[\Phi(t-\tau)\big]\big|\,|\Psi|\,\mathbf{d}\tau U \\ &= \int_{t_0}^{t} \mathbf{exp}\big[\Phi(t-\tau)\big]\mathbf{d}\tau\,|\Psi|\,U \\ &= \int_{0}^{t-t_0} \mathbf{exp}\big[\Phi s\big]\mathbf{d}s\,|\Psi|\,U \\ &= \frac{1}{\Phi}\left(\mathbf{exp}\big[\Phi(t-t_0)\big] - I_n\right)|\Psi|\,U = \gamma_M(t) \end{aligned}$$

The proof is complete.

In this paper, we consider the following LTI system with unknown but bounded uncertainties

$$\begin{aligned} x^{+}(t) &= Ax(t) + Bu(t) + d(t), \\ y(t) &= Cx(t) + n(t), \end{aligned} \tag{1}$$

where $x^{+}(t)$ represents $\dot{x}(t)$ in continuous time (CT) systems and $x(t+1)$ in discrete time (DT) systems. $x(t) \in \mathbb{R}^{n_x}$ is the state variable with initial condition $x(0) \in \big[\underline{x}_0, \overline{x}_0\big]$. The measured output $y(t) \in \mathbb{R}^{n_y}$ and control input $u(t) \in \mathbb{R}^{n_u}$ are governed by known constant coefficient matrices $A \in \mathbb{R}^{n_x \times n_x}$, $B \in \mathbb{R}^{n_x \times n_u}$, and $C \in \mathbb{R}^{n_y \times n_x}$. System disturbances $d(t) \in \mathbb{R}^{n_x}$ and measurement noises $n(t) \in \mathbb{R}^{n_y}$ are assumed to be within known bounds $d(t) \in [\underline{d}(t), \overline{d}(t)]$ and $n(t) \in [\underline{n}(t), \overline{n}(t)]$, with $\overline{d}(t) - \underline{d}(t) \le D$ and $\overline{n}(t) - \underline{n}(t) \le N$.

The uncertainties $d(t)$ and $n(t)$ can be reformulated as $d(t) = \frac{\overline{d}(t)+\underline{d}(t)}{2} + \tilde{d}(t)$ and $n(t) = \frac{\overline{n}(t)+\underline{n}(t)}{2} + \tilde{n}(t)$, where $\tilde{d}(t)$ and $\tilde{n}(t)$ are alternative uncertainties satisfying $\left|\tilde{d}(t)\right| \le \frac{D}{2}$ and $\left|\tilde{n}(t)\right| \le \frac{N}{2}$. Similarly, $\left|x(0) - \frac{\overline{x}_0+\underline{x}_0}{2}\right| \le \frac{\overline{x}_0-\underline{x}_0}{2} = X_0$, so that (1) can be equivalently transformed into

$$\begin{aligned} x^{+}(t) &= Ax(t) + \tilde{u}(t) + \tilde{d}(t), \\ \tilde{y}(t) &= Cx(t) + \tilde{n}(t), \end{aligned} \tag{2}$$

where $\tilde{u}(t) = Bu(t) + \frac{\underline{d}(t)+\overline{d}(t)}{2}$, $\tilde{y}(t) = y(t) - \frac{\underline{n}(t)+\overline{n}(t)}{2}$.

Our objective is to develop a fixed-time convergence-based ISE design technique to determine approximations of the upper and lower state bounds for the perturbed LTI system (1) at a pre-defined time.

3. Main results

With the coefficient matrices $R \in \mathbb{R}^{2n_x \times 2n_x}$, $L \in \mathbb{R}^{2n_x \times n_y}$, $K \in \mathbb{R}^{n_x \times 2n_x}$, and $T \in \mathbb{R}^{2n_x \times n_x}$, a scalar time delay $t_d > 0$, and along with a matrix function

$$\Upsilon(t) = \begin{cases} \mathbf{exp}\,[Rt] & \text{(CT)}, \\ R^t & \text{(DT)}, \end{cases}$$

a delay injection-based non-smooth auxiliary system for the variable $z(t)$ is constructed as follows:

$$z^{+}(t) = Rz(t) - L\tilde{y}(t) + T\tilde{u}(t), \tag{3}$$

$$\hat{x}(t) = K\left[z(t) - \Upsilon(t_d)z(t-t_d)\right], \tag{4}$$

where the operator $z^{+}(t)$ is analogous to $x^{+}(t)$, and the initial state is defined as:

$$z(t) = T\frac{\overline{x}_0 + \underline{x}_0}{2}, \quad -t_d \le t \le 0. \tag{5}$$

Define the estimation error as $e(t) = x(t) - \hat{x}(t)$. If the interval estimation $[\underline{e}(t), \overline{e}(t)]$ for $e(t)$ can be computed with fixed-time convergence, the Fixed-Time Interval State Estimation (F-ISE) for the system (1) is obtained as: $\overline{x}(t) = \hat{x}(t) + \overline{e}(t)$ and $\underline{x}(t) = \hat{x}(t) + \underline{e}(t)$. Based on the componentwise bound computation of the error $e(t)$, the F-ISE observer structure and its existence conditions for the system (1) are stated as follows.

Theorem 7. *Let* $\Pi = \begin{bmatrix} \frac{D}{2} \\ \frac{N}{2} \end{bmatrix}$, $\Delta = \begin{bmatrix} T & L \end{bmatrix}$ *and define the operator* $\gamma^{+}(t)$ *as the solution to:*

$$\dot{\gamma}(t) = \left|K\mathbf{exp}\left[Rt\right]\Delta\right|\Pi \quad \text{(CT)},$$

$$\gamma(t+1) = \left|K\sum_{i=0}^{t} R^i\Delta\right|\Pi \quad \text{(DT)},$$

and the piecewise function $E(t)$ *as*

$$E(t) = \begin{cases} |KT|X_0, & t = 0, \\ |K\Upsilon(t)T|X_0 + \gamma^{+}(t), & 0 < t < t_d, \\ \gamma^{+}(t_d), & t \ge t_d. \end{cases} \tag{6}$$

Then, the dynamic system defined by Eqs. (3)–(5) and

$$\overline{x}(t) = \hat{x}(t) + E(t), \quad \underline{x}(t) = \hat{x}(t) - E(t), \tag{7}$$

can achieve a stable F-ISE for the linear time-invariant (LTI) system (1) within the time t_d*, provided the coefficients* R, L, K, T*, and* $t_d > 0$ *satisfy the following conditions:*

$$TA + LC = RT, \tag{8}$$

$$K\begin{bmatrix} T & \Upsilon(t_d)T \end{bmatrix} = \begin{bmatrix} I_{n_x} & 0 \end{bmatrix}, \tag{9}$$

and R *is a stable matrix.*

Proof. Denote $\tilde{e}(t) = Tx(t) - z(t)$. From (2)–(5), we obtain:

$$\tilde{e}(t) = \begin{cases} -T\frac{\overline{x}_0+\underline{x}_0}{2}, & -t_d \le t < 0, \\ \tilde{e}_0 = T\left(x(0) - \frac{\overline{x}_0+\underline{x}_0}{2}\right), & t = 0. \end{cases} \tag{10}$$

For $t > 0$, using (8), $\phi(t) = \begin{bmatrix} \tilde{d}(t) \\ \tilde{n}(t) \end{bmatrix}$ and $\Delta = \begin{bmatrix} T & L \end{bmatrix}$, we have:

$$\begin{aligned} &\tilde{e}^{+}(t) = TAx(t) + T\tilde{u}(t) + T\tilde{d}(t) - Rz(t) \\ &+ L\tilde{y}(t) - T\tilde{u}(t) = R\tilde{e}(t) - (RT - LC - TA)x(t) \\ &+ L\tilde{n}(t) + T\tilde{d}(t) = R\tilde{e}(t) + \Delta\phi(t), \end{aligned} \tag{11}$$

and in the CT system, the solution to (11) is

$$\tilde{e}(t) = \mathbf{exp}\left[Rt\right]\tilde{e}_0 + \int_0^t \mathbf{exp}\left[R(t-\tau)\right]\Delta\phi(\tau)\mathbf{d}\tau, \; t > 0. \tag{12}$$

Next, the estimated state $\hat{x}(t)$ can be expressed as:

$$\begin{aligned} &\hat{x}(t) = K\Big[Tx(t) - \tilde{e}(t) + \Upsilon(t_d)\tilde{e}(t-t_d) \\ &- \Upsilon(t_d)Tx(t-t_d)\Big] = KTx(t) + K\Upsilon(t_d)\tilde{e}(t-t_d) \\ &- K\tilde{e}(t) - K\Upsilon(t_d)Tx(t-t_d) = K\Upsilon(t_d)\tilde{e}(t-t_d) \\ &+ K\begin{bmatrix} T & \Upsilon(t_d)T \end{bmatrix}\begin{bmatrix} x(t) \\ -x(t-t_d) \end{bmatrix} - K\tilde{e}(t). \end{aligned} \tag{13}$$

Then, from (9), the above Eq. (13) can be rewritten as $\hat{x}(t) = x(t) + K\Upsilon(t_d)\tilde{e}(t-t_d) - K\tilde{e}(t)$, that is

$$e(t) = K\tilde{e}(t) - K\Upsilon(t_d)\tilde{e}(t-t_d). \tag{14}$$

Substituting (9), (10) and (12) into (14), we derive $e(t)$ for the CT system as follows:

- For $t = 0$:

$$\begin{aligned} e(0) &= K\tilde{e}(0) - K\Upsilon(t_d)\tilde{e}(-t_d) \\ &= K\tilde{e}(0) + K\Upsilon(t_d)T\frac{\overline{x}_0 + \underline{x}_0}{2} = K\tilde{e}_0; \end{aligned}$$

- For $0 < t < t_d$:

$$\begin{aligned} e(t) &= K\mathbf{exp}\left[Rt\right]\tilde{e}_0 + K\int_0^t \mathbf{exp}\left[R(t-\tau)\right]\Delta\phi(\tau)\mathbf{d}\tau \\ &+ K\Upsilon(t_d)T\frac{\overline{x}_0 + \underline{x}_0}{2} = K\mathbf{exp}\left[Rt\right]\tilde{e}_0 \\ &+ K\int_0^t \mathbf{exp}\left[R(t-\tau)\right]\Delta\phi(\tau)\mathbf{d}\tau; \end{aligned}$$

- For $t \geq t_d$:

$$\begin{aligned} e(t) &= K\mathbf{exp}\big[Rt\big]\tilde{e}_0 + K\int_0^t \mathbf{exp}\big[R(t-\tau)\big]\Delta\phi(\tau)\mathbf{d}\tau \\ &- K\Upsilon(t_d)\mathbf{exp}\big[R(t-t_d)\big]\tilde{e}_0 \\ &- K\Upsilon(t_d)\int_0^{t-t_d} \mathbf{exp}\big[R(t-t_d-\tau)\big]\Delta\phi(\tau)\mathbf{d}\tau \\ &= K\mathbf{exp}\big[Rt\big]\tilde{e}_0 + K\int_0^t \mathbf{exp}\big[R(t-\tau)\big]\Delta\phi(\tau)\mathbf{d}\tau \\ &- K\mathbf{exp}\big[Rt\big]\tilde{e}_0 - K\int_0^{t-t_d} \mathbf{exp}\big[R(t-\tau)\big]\Delta\phi(\tau)\mathbf{d}\tau \\ &= K\int_0^t \mathbf{exp}\big[R(t-\tau)\big]\Delta\phi(\tau)\mathbf{d}\tau \\ &- K\int_0^{t-t_d} \mathbf{exp}\big[R(t-\tau)\big]\Delta\phi(\tau)\mathbf{d}\tau \\ &= K\int_{t-t_d}^t \mathbf{exp}\big[R(t-\tau)\big]\Delta\phi(\tau)\mathbf{d}\tau. \end{aligned}$$

For the DT system, the error $e(t)$ can be similarly derived:

$$e(t) = \begin{cases} K\tilde{e}(0), & t = 0, \\ KR^t\tilde{e}(0) + K\sum_{i=0}^{t-1} R^i\Delta\phi(t-1-i), & 0 < t < t_d, \\ K\sum_{i=0}^{t_d-1} R^i\Delta\phi(t-1-i), & t \geq t_d. \end{cases} \tag{15}$$

Using $|\phi(t)| \leq \Pi = \begin{bmatrix} \frac{D}{2} \\ \frac{N}{2} \end{bmatrix}$ and Lemma 6, the componentwise bound of $e(t)$ is computed as in (6). This implies: $\underline{x}(t) \leq x(t) \leq \overline{x}(t), \quad \forall t \geq 0$. From the stable matrix R and the fixed-time convergence property of $e(t)$, the ISE for $x(t)$ is guaranteed to converge within $t_d > 0$. Thus, the dynamic system (3)–(5) and (7) achieves a stable ISE for the system (1). The proof is complete.

Remark 8. When the time-delay property is not introduced, i.e., $t_d = +\infty$, we have $\Upsilon(t_d) = 0$ and $KT = I_{n_x}$. In this case, the error dynamics in the CT system simplifies to: $e(t) = K\mathbf{exp}\big[Rt\big]\tilde{e}(0)+K\int_0^t \mathbf{exp}\big[R(t-\tau)\big]\Delta\phi(\tau)\mathbf{d}\tau$, and in the DT system: $e(t) = KR^t\tilde{e}(0) + K\sum_{i=0}^{t-1} R^i\Delta\phi(t-1-i)$. Using the integral inequality for nonnegative vectors and Lemma 6, we can obtain $\lim_{t\to+\infty}|e(t)| \to \gamma^+(+\infty)$, and for any $t_d < +\infty$, $\gamma^+(t_d) < \gamma^+(+\infty)$. This demonstrates that under the conditions of (8) and (9), the F-ISE given by (3)–(5) and (7) provides a more accurate estimation compared to its exponentially convergent counterpart. In other words, among the same exponentially convergent observer structure, the delay-injection mechanism reduces the estimation conservatism.

From Theorem 7, the bound computation-based F-ISE (BC-FISE) implementation is equivalent to solving the matrix equations (MEs) (8) and (9) with the constraint on R. By solving this MEs, we propose a feasibility parametric design method for the system defined by (3)–(5) and (7), as described below.

Theorem 9. *Given the right coprime polynomial matrices $X(s) = \sum_{j=0}^{\varpi} X_j s^j$ and $Y(s) = \sum_{j=0}^{\varpi} Y_j s^j$ on the coefficient s of the matrix pair $(A^{\mathrm{T}}, C^{\mathrm{T}})$, where ϖ is the maximum degree between $Y(s)$ and $X(s)$, and denoting R^j as the jth matrix power of R with $R^0 = I_{2n_x}$, a set of feasible solutions to the BC-FISE (3)–(5) and (7) for the observable system (1) is obtained as:*

$$T = \sum_{j=0}^{\varpi} R^j Z^{\mathrm{T}} X_j^{\mathrm{T}}, L = \sum_{j=0}^{\varpi} R^j Z^{\mathrm{T}} Y_j^{\mathrm{T}}, \tag{16a}$$

$$K = \begin{bmatrix} I_{n_x} & 0 \end{bmatrix}\begin{bmatrix} T & \Upsilon(t_d)T \end{bmatrix}^{-1}, \tag{16b}$$

if there exists a stable R, a parameter $Z \in \mathbb{R}^{n_y\times 2n_x}$, and a time-delay t_d satisfying:

$$\mathbf{rank}\begin{bmatrix} T & \Upsilon(t_d)T \end{bmatrix} = 2n_x. \tag{17}$$

Proof. Since the dual system of an observable pair (C, A) is controllable, there must be a pair of right coprime polynomial matrices $X(s)$ and $Y(s)$ satisfying $\big(sI_{n_x} - A^{\mathrm{T}}\big)X(s) - C^{\mathrm{T}}Y(s) = 0$. According to the works in Duan (2015), Liu et al. (2023a), the parametric solutions to the matrix Eq. (8) exist in the form (16a), subject to the free parameters R and $Z \in \mathbb{R}^{n_y\times 2n_x}$. With a stable R, the parameter Z, and the time-delay t_d satisfying (17), the solution K to (9) can be computed as (16b). The proof is complete.

The following lemma is introduced to supports that the BC-FISE parametric design in Theorem 9 is always feasible for an observable pair $\big(C, A\big)$ and for almost all $t_d > 0$ (in CT systems) or $t_d > 1$ (in DT systems).

Lemma 10. *For almost all $t_d > 0$ in the CT systems or $t_d > 1$ in the DT systems, a solution to the matrix Eqs. (8) and (9) with a stable R always exists for an observable pair $\big(C, A\big)$.*

Proof. The matrices T, L, R, and K from Theorem 7 can be chosen as required, as it will be shown below. Suppose that T is column-full rank. Then there exists a nonsingular matrix $V \in \mathbb{R}^{2n_x\times 2n_x}$ such that $VT = \begin{bmatrix} I_{n_x} \\ I_{n_x} \end{bmatrix}$. Denoting $L = V^{-1}\begin{bmatrix} \tilde{L}_1 \\ \tilde{L}_2 \end{bmatrix}$, where $\tilde{L}_i \in \mathbb{R}^{n_x\times n_y}, i = 1, 2$, and left-multiplying (8) by V, the equation can be rewritten as:

$$VTA + VLC = \begin{bmatrix} A \\ A \end{bmatrix} + \begin{bmatrix} \tilde{L}_1 C \\ \tilde{L}_2 C \end{bmatrix} = VRV^{-1}\begin{bmatrix} I_{n_x} \\ I_{n_x} \end{bmatrix}. \tag{18}$$

It is straightforward to show that a set of solutions to (18) exists as: $R = V^{-1}\begin{bmatrix} A + \tilde{L}_1 C & 0 \\ 0 & A + \tilde{L}_2 C \end{bmatrix} V$, where $\tilde{L}_i, i = 1, 2$ are free parameters. Since (C, A) is an observable pair, the eigenvalues of R can be assigned arbitrarily by designing $\tilde{L}_i$. Thus, the matrix Eq. (8) always has a solution for V, L, and a stable R.

Further, let $\tilde{\Upsilon}_i(t_d) = \mathbf{exp}\big[(A + \tilde{L}_i C)t_d\big]$ in the CT systems or $\tilde{\Upsilon}_i(t_d) = (A + \tilde{L}_i C)^{t_d}$ in the DT systems. The operator $\Upsilon(t_d)$ can be rewritten as $V^{-1}\begin{bmatrix} \tilde{\Upsilon}_1(t_d) & 0 \\ 0 & \tilde{\Upsilon}_2(t_d) \end{bmatrix} V$. Denote $K = \begin{bmatrix} \tilde{K}_1 & \tilde{K}_2 \end{bmatrix} V$, where $\tilde{K}_i \in \mathbb{R}^{n_x\times n_x}, i = 1, 2$. From (9), we have $\tilde{K}_1 = I_{n_x} - \tilde{K}_2$ and $\tilde{K}_2\big(\tilde{\Upsilon}_1(t_d) - \tilde{\Upsilon}_2(t_d)\big) = \tilde{\Upsilon}_1(t_d)$, and following (Engel & Kreisselmeier, 2002; Zhang et al., 2019) and given two scalars $\sigma_1 > 0$, $0 < \sigma_2 < 1$, easy to deduced that when we choose $\tilde{L}_i, i = 1, 2$ such that $\mathbf{Re}\Big[\lambda_j(A + \tilde{L}_2 C)\Big] < \sigma_1 < \mathbf{Re}\Big[\lambda_j(A + \tilde{L}_1 C)\Big] < 0, j = 1, 2, \ldots, n_x$ holds in the CT systems or $\Big|\lambda_j(A + \tilde{L}_2 C)\Big| < \sigma_2 < \Big|\lambda_j(A + \tilde{L}_1 C)\Big| < 1, j = 1, 2, \ldots, n_x$ holds in the DT systems, the rank condition $\mathbf{rank}\big(\tilde{\Upsilon}_1(t_d) - \tilde{\Upsilon}_2(t_d)\big) = n_x$ holds for almost all $t_d > 0$ in the CT systems or $t_d > 1$ in the DT systems, which implies that Eq. (9) always has a solution for $\tilde{K}_i, i = 1, 2$. Therefore, the solution to the matrix Eqs. (8) and (9) with the constraint on R always exists for an observable pair $\big(C, A\big)$. The proof is complete.

Then, the BC-FISE for the system (1) can be implemented using Algorithm 1.

Remark 11. From (6) and (7), the componentwise bound of the F-ISE total error interval is given as $\bar{\gamma}(K, R, T, L) = \overline{x}(t) - \underline{x}(t) = 2\gamma^+(t_d)$. In the CT systems, using the trapezoidal approximation for the integral operation, $\gamma^+(t_d)$ can be approximated

Algorithm 1 BC-FISE Design Procedure.

Input: $A, B, C, D, N, u, y, [\underline{d}, \overline{d}], [\underline{n}, \overline{n}], [\underline{x}_0, \overline{x}_0], t_d$;
Output: $\overline{x}(t), \underline{x}(t)$;
1: Compute the observability matrix:

$$\mathcal{O} \leftarrow \begin{bmatrix} C^{\mathrm{T}} & A^{\mathrm{T}}C^{\mathrm{T}} & \cdots & (A^{n_x-1})^{\mathrm{T}}C^{\mathrm{T}} \end{bmatrix}^{\mathrm{T}};$$

2: **If rank** $\mathcal{O} = n_x$ **then**
3: Calculate the right coprim polynomial matrices $X(s), Y(s)$ for the pair $(A^{\mathrm{T}}, C^{\mathrm{T}})$;
4: Select stable R and parameter Z as in (17);
5: Compute:

$$T \leftarrow \sum_{j=0}^{\varpi} R^j Z^{\mathrm{T}} X_j^{\mathrm{T}}, L \leftarrow \sum_{j=0}^{\varpi} R^j Z^{\mathrm{T}} Y_j^{\mathrm{T}};$$

$$K \leftarrow \begin{bmatrix} I_{n_x} & 0 \end{bmatrix} \begin{bmatrix} T & \Upsilon(t_d)T \end{bmatrix}^{-1};$$

6: Define:

$$z(t) \leftarrow \begin{cases} z^+(t) = Rz(t) - L\tilde{y}(t) + T\tilde{u}(t), & t > 0, \\ T\frac{\overline{x}_0 + \underline{x}_0}{2}, & -t_d \le t \le 0; \end{cases}$$

7: Compute:

$$\hat{x}(t) \leftarrow K\left[z(t) - \Upsilon^+(t_d)z(t-t_d)\right];$$

8: Evaluate:

$$E(t) \leftarrow \begin{cases} |KT|X_0, & t = 0, \\ |K\Upsilon(t)T|X_0 + \gamma^+(t), & 0 < t < t_d, \\ \gamma^+(t_d), & t \ge t_d; \end{cases}$$

9: Compute interval bounds:

$$\overline{x}(t) \leftarrow \hat{x}(t) + E(t), \ \underline{x}(t) \leftarrow \hat{x}(t) - E(t);$$

10: **Else**
11: Output: No Solution;
12: **EndIf**

as: $\gamma^+(t_d) \approx \frac{t_d}{2n}\left(|K\mathbf{exp}[Rt_d]\Delta| + 2\sum_{k=1}^{n-1}\left|K\mathbf{exp}\left[R\frac{t_d}{n}k\right]\Delta\right|\right)\Pi$. Under (16), this can be reformulated into the parametric form $\bar{\gamma}(R, Z) = [\gamma_i(R, Z)] \in \mathbb{R}^{n_x}$, revealing available degrees of freedom and the numerical correlation between observer performance and design parameters. By minimizing the index $J = \sum_{i=1}^{n_x} \alpha_i\gamma_i(R, Z)$, where α_i are componentwise weights ($\sum_{i=1}^{n_x} \alpha_i = 1$), the F-ISE performance can be improved, emphasizing a purposeful design objective and providing greater flexibility for designers.

4. Extension and comparison analysis

Inspired by the delay injection-based non-smooth framework (3)–(5), a monotone system-based fixed-time interval observer (MS-FIO) can be formulated as follows:

$$\begin{cases} \overline{z}^+(t) = R\overline{z}(t) - Ly(t) + TBu(t) + \overline{\phi}(t), \\ \underline{z}^+(t) = R\underline{z}(t) - Ly(t) + TBu(t) + \underline{\phi}(t), \end{cases} \tag{19}$$

$$\begin{cases} \bar{\hat{x}}(t) = \overline{z}(t) - \Upsilon(t_d)\overline{z}(t-t_d), \\ \underline{\hat{x}}(t) = \underline{z}(t) - \Upsilon(t_d)\underline{z}(t-t_d), \\ \overline{x}^M(t) = K^{\mathrm{u}}\bar{\hat{x}}(t) - K^{\mathrm{d}}\underline{\hat{x}}(t), \\ \underline{x}^M(t) = K^{\mathrm{u}}\underline{\hat{x}}(t) - K^{\mathrm{d}}\bar{\hat{x}}(t), \end{cases} \tag{20}$$

Here, the operators $\overline{z}^+(t)$ and $\underline{z}^+(t)$ are the same as $z^+(t)$. The terms $\overline{\phi}(t)$ and $\underline{\phi}(t)$ are defined as: $\overline{\phi}(t) = T^{\mathrm{u}}\overline{d}(t) - T^{\mathrm{d}}\underline{d}(t) + L^{\mathrm{u}}\overline{n}(t) - L^{\mathrm{d}}\underline{n}(t)$, $\underline{\phi}(t) = T^{\mathrm{u}}\underline{d}(t) - T^{\mathrm{d}}\overline{d}(t) + L^{\mathrm{u}}\underline{n}(t) - L^{\mathrm{d}}\overline{n}(t)$.

The initial states are chosen for any vector z_0 as:

$$\begin{bmatrix} \overline{z}(t) \\ \underline{z}(t) \end{bmatrix} = \begin{cases} \begin{bmatrix} T^+\overline{x}_0 - T^-\underline{x}_0 \\ T^+\underline{x}_0 - T^-\overline{x}_0 \end{bmatrix}, & t = 0, \\ \begin{bmatrix} Tz_0 \\ Tz_0 \end{bmatrix}, & -t_d \le t < 0. \end{cases} \tag{21}$$

Next, a parametric design method for the interval observer (19)–(21), along with its performance comparison to the F-ISE (3)–(5), (7), is presented below.

Theorem 12. *A stable MS-FIO (19)–(21) within a predefined time delay $t_d > 0$ for the LTI system (1) can be designed by (16), if the following conditions are satisfied: R is both stable and monotone and the parameters R and Z satisfy (17). Besides, the above MS-FIO and the BC-FISE satisfy the inequalities $\overline{x}(t) \le \overline{x}^M(t)$ and $\underline{x}(t) \ge \underline{x}^M(t)$ under the same R and Z.*

Proof. Utilizing the solutions for the states $\bar{\overline{e}}(t) = \overline{z}(t) - Tx(t)$, $\underline{\bar{e}}(t) = Tx(t) - \underline{z}(t)$, and the inputs $\overline{\Phi}(t) = \overline{\phi}(t) - Td(t) - Ln(t)$, $\underline{\Phi}(t) = Td(t) + Ln(t) - \underline{\phi}(t)$, and referring to the proof process in Theorem 7, we derive the piecewise representations of $\overline{e}(t) = \overline{x}^M(t) - x(t)$ and $\underline{e}(t) = x(t) - \underline{x}^M(t)$. Using monotone system theory, we deduce that the inequality $\underline{x}^M(t) \le x(t) \le \overline{x}^M(t)$ holds for all $t \ge 0$, with fixed-time convergence at t_d, provided that the matrix Eqs. (8) and (9) have solutions for a stable and monotone R.

Applying a similar deduction process as in Theorem 9 confirms the first part of this theorem. To save space, the detailed proof is omitted.

Next, let $z_0 = \frac{\overline{x}_0 + \underline{x}_0}{2}$, and define $\bar{e}_z(t) = \overline{z}(t) - z(t)$. From (3) and (19), we obtain:

$$\begin{aligned} &\bar{e}_z(t) = 0, \quad -t_d \le t < 0, \quad \bar{e}_z(0) = |T|X_0, \\ &\bar{e}_z^+(t) = R\overline{z}(t) - Ly(t) + TBu(t) + \overline{\phi}(t) - Rz(t) + L\tilde{y}(t) \\ &- T\tilde{u}(t) = R\bar{e}_z(t) + \overline{\phi}(t) - L\frac{\underline{n}(t) + \overline{n}(t)}{2} - T\frac{\underline{d}(t) + \overline{d}(t)}{2}, \\ &= R\bar{e}_z(t) + |L|\frac{N}{2} + |T|\frac{D}{2} = R\bar{e}_z(t) + |\Delta|\,\Pi, \quad t > 0. \end{aligned}$$

The solutions in the CT and DT systems are given as:

$$\bar{e}_z(t) = \begin{cases} \mathbf{exp}\left[Rt\right]\bar{e}_z(0) + \frac{1}{R}\left(\mathbf{exp}\left[Rt\right] - I_{2n_x}\right)|\Delta|\,\Pi, & \text{(CT)}, \\ R^t\bar{e}_z(0) + \sum_{i=0}^{t-1} R^i\,|\Delta|\,\Pi, & \text{(DT)}. \end{cases} \tag{22}$$

Following a similar derivation for $\underline{e}_z(t) = z(t) - \underline{z}(t)$, we find $\underline{e}_z(t) = \bar{e}_z(t)$ for all $t \ge -t_d$.

From (20), define $\bar{e}_M(t) = \overline{x}^M(t) - \hat{x}(t)$. Then:

$$\begin{aligned} \bar{e}_M(t) &= K^{\mathrm{u}}\bar{\hat{x}}(t) - K^{\mathrm{d}}\underline{\hat{x}}(t) - \hat{x}(t) = K^{\mathrm{u}}\bar{e}_z(t) + K^{\mathrm{d}}\underline{e}_z(t) \\ &\quad - K^{\mathrm{u}}\Upsilon^+(t_d)\bar{e}_z(t-t_d) - K^{\mathrm{d}}\Upsilon(t_d)\underline{e}_z(t-t_d), \\ &= |K|\,\bar{e}_z(t) - |K|\,\Upsilon(t_d)\bar{e}_z(t-t_d). \end{aligned} \tag{23}$$

Substituting (22) into (23) above yields:

$$\bar{e}_M(t) = \begin{cases} |K|\,|T|X_0, & t = 0, \\ |K|\,\Upsilon^+(t)\,|T|X_0 + \gamma_M^+(t), & 0 < t < t_d, \\ \gamma_M^+(t_d), & t \ge t_d, \end{cases}$$

where $\gamma_M^+(t)$ denotes $|K|\,\frac{1}{R}\left(\mathbf{exp}\left[Rt\right] - I_n\right)|\Delta|\,\Pi$ and $|K|\sum_{i=0}^{t-1}\Upsilon^+(i)\,|\Delta|\,\Pi$ in the CT and DT systems, respectively. Using the same solutions (16) for both the bound computation-based F-ISE (3)–(5),

(7) and the MS-FIO (19)–(21), and based on Lemma 6, we have $\bar{e}_M(t) \ge E(t)$ for all $t \ge 0$, implying $\bar{x}^M(t) - \bar{x}(t) \ge 0$, i.e., $\bar{x}(t) \le \bar{x}^M(t)$. Similarly, we can show $\underline{x}(t) \ge \underline{x}^M(t)$. Both parts of this theorem are complete.

In view of the work (Huang et al., 2021; Tang et al., 2019), the set propagation-based F-ISE (SP-FISE), which leverages reachability analysis and zonotopes using the non-smooth observer (3)–(5) as a propagation carrier, is introduced and compared in terms of performance below.

Theorem 13. *For the DT LTI system (1), the state $x(t)$ can be bounded as $\bar{x}^S(t) = \hat{x}(t) + \bar{E}(t)$ and $\underline{x}^S(t) = \hat{x}(t) + \underline{E}(t)$ with (3)–(5), $\left[\underline{E}(t), \bar{E}(t)\right] = \mathbf{Hull}\left[\mathbf{E}^S(t)\right]$, with*

$$\mathbf{E}^S(t) = \begin{cases} KT \odot \mathbf{X}_0, & t = 0, \\ KR^t T \odot \mathbf{X}_0 \oplus \bigoplus_{i=0}^{t-1} KR^i \Delta \odot \mathbf{U}, & 0 < t < t_d, \\ \bigoplus_{i=0}^{t_d-1} KR^i \Delta \odot \mathbf{U}, & t \ge t_d, \end{cases} \tag{24}$$

where Π, Δ, T, L, R, and K are as defined and computed in Theorems 7 and 9, and $\mathbf{U} = \langle 0, \mathbf{diag}[\Pi] \rangle$, $\mathbf{X}_0 = \langle 0, \mathbf{diag}[X_0] \rangle$. Besides, the above SP- and BC-FISEs satisfy the equations $\bar{x}(t) = \bar{x}^S(t)$ and $\underline{x}(t) = \bar{x}^S(t)$ under the same R and Z.

Proof. Given the equivalent LTI system (2), it holds that $\tilde{n}(t) \in \langle 0, \mathbf{diag}[\frac{N}{2}] \rangle$, $\tilde{d}(t) \in \langle 0, \mathbf{diag}[\frac{D}{2}] \rangle$, and $x(0) - \frac{\bar{x}_0 + \underline{x}_0}{2} \in \langle 0, \mathbf{diag}[X_0] \rangle$. Using the reachable set of $e(t)$ as given in (15), we compute the reachable set $\mathbf{E}^S(t)$ in (24), and the interval range is obtained as $\left[\underline{E}(t), \bar{E}(t)\right] = \mathbf{Hull}\left[\mathbf{E}^S(t)\right]$. Thus, since $e(t) \in \mathbf{E}^S(t) \subseteq \mathbf{Hull}\left[\mathbf{E}^S(t)\right]$, it follows that $\underline{E}(t) \le e(t) \le \bar{E}(t)$ for all t, which implies $\underline{x}^S(t) \le x(t) \le \bar{x}^S(t)$ for all t. When uncertainties are not considered, $e(t) = 0$ for $t \ge t_d$. Furthermore, under the **Hull** operator and the same R and Z, we have $\underline{E}(t) = -\bar{E}(t) = E(t)$, which gives $\bar{x}(t) = \bar{x}^S(t)$ and $\underline{x}(t) = \bar{x}^S(t)$. The proof is complete.

Theorem 12 demonstrates that, within the same delay injection-based framework, the BC-FISE (3)–(5), (7) outperforms the MS-FIO both in performance and design constraints. According to Lemma 10, the additional design constraints for MS-FIO can lead to feasibility issues under an observable pair (C, A). Although coordinate transformations may resolve these issues, they introduce additional complexities, conservatism, and computational errors.

Theorem 13 also indicates that the BC- and SP-FISEs exhibit the same estimation performance, with the latter limited to DT systems. Inspired by Xu, Yang, and Liang (2020a, 2020b) and the extensions in this paper (Theorems 12 and 13), a fixed-time set-theoretic interval observer design can be achieved using the delay injection-based framework, extendable to CT systems via Euler discretization. This tradeoff solution, however, has higher design and estimation conservatism than Theorem 7.

Finally, for interval state estimation objectives (e.g., $L = I_{n_x}$ as in Liu et al. (2020)), the delay injection-based framework imposes no constraints on the derivative (or differential) term of the measurement noise $n(t)$, the system matrix A, the fixed-time convergence rate, or the observer system matrix R. This flexibility ensures broader applicability and richer design parameters compared to existing methods (Dinh et al., 2019, 2020; Khan et al., 2021, 2020; Liu et al., 2020; Meslem & Ramdani, 2020; Wang, Dinh et al., 2022a). Moreover, Theorem 7 provides interval estimates for $x(t)$ before the fixed-time constant, offering a wider range of fault monitoring than the methods in Dinh et al. (2019, 2020), Wang, Dinh et al. (2022a).

5. Simulation examples

Two examples, one CT system and one DT system, are provided to illustrate the validity and superiority of the proposed results.

5.1. Example 1

Consider a CT system (1) with $u(t) = 3\sin(t) - 2\sin(3t)$, $d(t) = 0.1\begin{bmatrix}\mathbf{r}(t) & \mathbf{r}(t) & 2\mathbf{r}(t)\end{bmatrix}^{\mathrm{T}}$, $n(t) = 0.1\begin{bmatrix}1 & 1\end{bmatrix}^{\mathrm{T}}\sin^3(t)$ and $A = \begin{bmatrix}-1 & -3 & 5 \\ 0 & 1 & -3 \\ 0 & 2 & -2\end{bmatrix}$, $B = \begin{bmatrix}-5 \\ 1 \\ -1\end{bmatrix}$, $C = \begin{bmatrix}-1 & -2 & 1 \\ 0 & 1 & 0\end{bmatrix}$. Here, $-1 < \mathbf{r}(t) < 1$ is a random number dependent on t, and the uncertainties $d(t), n(t), \dot{n}(t)$, and the initial states $x(0)$ are bounded by $\bar{d}(t) = \begin{bmatrix}0.1 & 0.1 & 0.2\end{bmatrix}^{\mathrm{T}}$, $\underline{d}(t) = -\bar{d}(t)$, $\bar{n}(t) = \begin{bmatrix}0.1 & 0.1\end{bmatrix}^{\mathrm{T}}$, $\underline{n}(t) = -\bar{n}(t)$, $\bar{x}_0 = \begin{bmatrix}0 & 1 & 2\end{bmatrix}^{\mathrm{T}}$, $\underline{x}_0 = \begin{bmatrix}-2 & -1 & 0\end{bmatrix}^{\mathrm{T}}$, $\bar{n}_d(t) = \begin{bmatrix}0.3 & 0.3\end{bmatrix}^{\mathrm{T}}$, $\underline{n}_d(t) = -\bar{n}_d(t)$. Since the system is observable, the F-ISE (3)–(5) and (7) can be designed by Theorem 9 with $t_d = 0.5$ and

$$R = \mathbf{diag}\left[-1, -2, -3, -6, -7, -8\right], \quad Z = \begin{bmatrix}0.5 & 0.5 & 0.5 & 0.5 & -0.5 & 0.5 \\ 0.5 & -0.5 & 0.5 & 0.5 & 0.5 & 0.5\end{bmatrix}. \tag{25}$$

Because the second state $x_2(t)$ can be directly obtained from the measured output, we focus on the states $x_1(t)$ and $x_3(t)$ as the main observation targets. Simulation results are shown in Fig. 1. The MS-FIO from Liu et al. (2020), Theorem 9 with $t_d = +\infty$, Theorem 12 with the same R and Z as in (25), and the optimal MS-IOs from Liu et al. (2023b), Wang, Yin et al. (2022b) are included for comparison. All ISEs achieve stable upper and lower bound estimations for $x_1(t)$ and $x_3(t)$. The F-ISEs proposed in Liu et al. (2020) and Theorems 9 and 12 achieve steady-state estimations within the fixed-time delay t_d. Additionally, Theorem 9 demonstrates superior accuracy compared to optimized ISEs (Liu et al., 2023b; Wang, Yin et al., 2022b). These results confirm that Theorem 9 delivers the best performance among these methods.

5.2. Example 2

Consider a DT nonlinear system (1) with: $A = \begin{bmatrix}0 & 0 & 0 & 0 \\ 1 & 0 & 0 & 0 \\ 0 & 0.5 & 0 & 0 \\ 0 & 0 & -1 & 0\end{bmatrix}$, $B = \begin{bmatrix}1.25 \\ 0 \\ 1 \\ 0\end{bmatrix}$, $C = \begin{bmatrix}1 & 0 & 0 & 0 \\ 0 & 0 & 1 & 0 \\ 0 & 0 & 0 & 1\end{bmatrix}$, $d(x_2, t) = \begin{bmatrix}0.1 & 0.1 & -0.1 & -0.2\end{bmatrix}^{\mathrm{T}} \sin(2t) + \begin{bmatrix}0.1\sin(x_2(t)) & 0 & 0 & 0\end{bmatrix}^{\mathrm{T}}$, $u(t) = 3\sin(2t)$, $n(t) = \begin{bmatrix}0.1 & 0.1 & 0.1\end{bmatrix}^{\mathrm{T}}\mathbf{r}(t)$, where $\mathbf{r}(t)$ represents a random sequence. It is easy to verify that the above uncertain system is observable, but $\mathbf{rank}(A) \ne n_x$. Consequently, this system is outside the application scope of the methods presented in Dinh et al. (2019), Meslem and Ramdani (2020), Wang, Dinh et al. (2022a). Using Theorems 9, we compute the solutions T, L, K to (8) and (9) with $t_d = 2 < n_x - 1 = 3$, using a stable and monotone matrix:

$$R = \left[\begin{array}{c:cccc} & 0 & 0 & 0.2 & 0 \\ R_1 & 0 & 0 & 0 & 0.1 \\ & 0 & 0 & 0.1 & 0 \\ & 0 & 0 & 0 & 0 \\ \hdashline 0 & & & R_2 & \end{array}\right],$$

where $R_1 = \mathbf{diag}\left[0.1, 0.1, 0.2, 0.1\right]$ and $R_2 = \mathbf{diag}\left[0.9, 0.7, 0.9, 0.7\right]$. This matrix is applied for Theorems 9, 12, and 13. Note

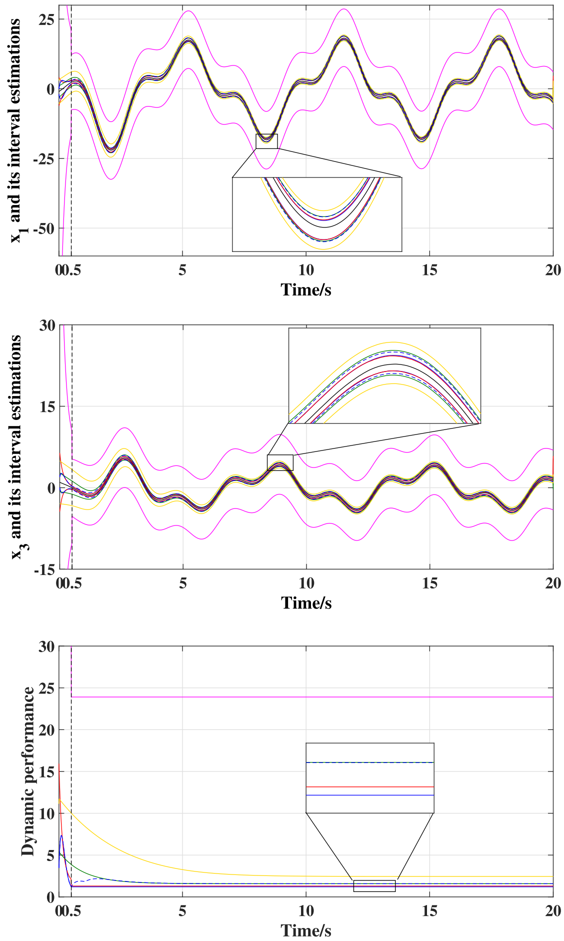

Fig. 1. ISEs for $x_1(t)$ and $x_3(t)$ and their dynamic performance (Wang, Yin et al., 2022b): black lines represent system states; yellow, green, red, pink, and blue (solid/dotted) lines represent results from Liu et al. (2020, 2023b), Wang, Yin et al. (2022b), Theorem 12, and Theorem 9, respectively.

that the matrix R is not in block diagonal form, as seen in Liu et al. (2020).

To effectively distinguish Theorems 12 and 13, we assign different initial states for them. The simulation results are presented in Fig. 2. As shown, Theorem 9 outperforms Theorem 12 and exhibits equivalent performance to Theorem 13, which is consistent with the analysis in Section 4.

6. Conclusion

In this paper, a unified F-ISE design framework for both CT and DT systems is presented, leveraging a novel delay injection-based non-smooth observer structure. The existence conditions and parametric expressions are systematically derived under the common observability condition. This F-ISE design method significantly relaxes many of the design and estimation constraints found in existing approaches and provides a clear explanation of the numerical correlation between observer performance and design parameters. Furthermore, compared to its extensions based on IO-ISE and SP-ISE, the proposed method demonstrates a broader application scope and achieves more accurate estimation performance under identical parameter settings. Finally, two simulations are provided to validate and support these findings effectively. Future work will explore the address sensitivity in algebraic approach and its further extension to more complex systems.

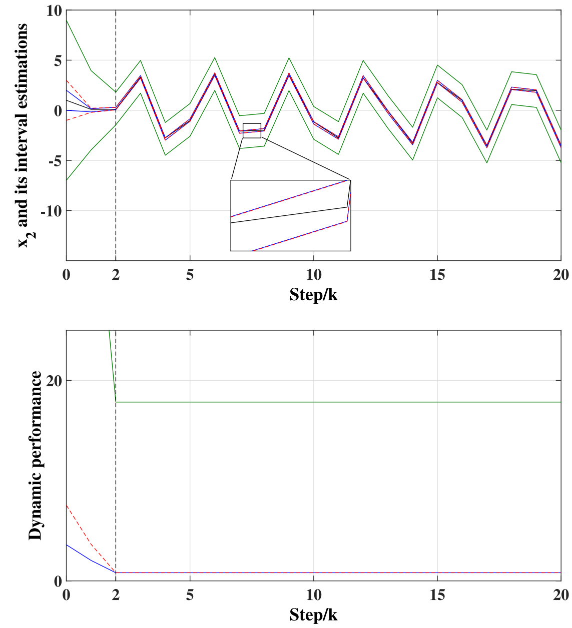

Fig. 2. ISEs for $x_2(t)$ and their dynamic performance (Wang, Yin et al., 2022b): black lines represent the system states, red lines are provided by Theorem 13, green lines are provided by Theorem 12, and blue lines are provided by Theorem 9.

Acknowledgments

A part of the work was done during Thach Ngoc Dinh's stay at the Vietnam Institute for Advanced Study in Mathematics in Hanoi. He is grateful to the Institute for its hospitality and supportive environment.

References

Alamo, T., Bravo, J. M., & Camacho, E. F. (2005). Guaranteed state estimation by zonotopes. *Automatica*, *41*(6), 1035–1043.

Althoff, M., & Rath, J. J. (2021). Comparison of guaranteed state estimators for linear time-invariant systems. *Automatica*, *130*, Article 109662.

Chisci, L., Garulli, A., & Zappa, G. (1996). Recursive state bounding by parallelotopes. *Automatica*, *32*(7), 1049–1055.

Dinh, T. N., Mazenc, F., & Raïssi, T. (2019). Finite-time guaranteed state estimation for discrete-time systems with disturbances. In *IEEE conference on control and fault tolerant systems* (pp. 342–347). IEEE.

Dinh, T. N., Mazenc, F., Wang, Z., & Raissi, T. (2020). On fixed-time interval estimation of discrete-time nonlinear time-varying systems with disturbances. In *American control conference* (pp. 2605–2610). IEEE.

Duan, G.-R. (2015). *Generalized sylvester equations/g*. Boca Raton, FL: CRC Press.

Efimov, D., & Raïssi, T. (2016). Design of interval observers for uncertain dynamical systems. *Automation and Remote Control*, *77*, 191–225.

Engel, R., & Kreisselmeier, G. (2002). A continuous-time observer which converges in finite time. *IEEE Transactions on Automatic Control*, *47*(7), 1202–1204.

Ethabet, H., Rabehi, D., Efimov, D., & Raïssi, T. (2018). Interval estimation for continuous-time switched linear systems. *Automatica*, *90*, 230–238.

Gouzé, J.-L., Rapaport, A., & Hadj-Sadok, M. Z. (2000). Interval observers for uncertain biological systems. *Ecological Modelling*, *133*(1–2), 45–56.

Huang, J., Che, H., Raïssi, T., & Wang, Z. (2021). Functional interval observer for discrete-time switched descriptor systems. *IEEE Transactions on Automatic Control*, *67*(5), 2497–2504.

Huang, J., Yu, S., Ma, X., & Chen, L. (2018). Finite time interval observer design for discrete-time switched systems. In *International symposium on positive systems* (pp. 73–82). Springer.

Kalman, R. E. (1960). A new approach to linear filtering and prediction problems. *Journal of Basic Engineering*, *82D*, 35–45.

Khan, A., Bai, X., Zhang, B., & Yan, P. (2021). Interval state estimator design for linear parameter varying (lpv) systems. *IEEE Transactions on Circuits and Systems II: Express Briefs*, *68*(8), 2865–2869.

Khan, A., Xie, W., & Liu, L.-W. (2020). Set-membership interval state estimator design using observability matrix for discrete-time switched linear systems. *IEEE Sensors Journal*, *20*(11), 6121–6129.
Liu, L.-W., Xie, W., Khan, A., & Zhang, L.-W. (2020). Finite-time functional interval observer for linear systems with uncertainties. *IET Control Theory & Applications*, *14*(18), 2868–2878.
Liu, L.-W., Xie, W., & Zhang, L.-W. (2023a). Luenberger-type interval observer for continuous-time perturbed singular systems. *Systems & Control Letters*, *173*, Article 105484.
Liu, L.-W., Xie, W., & Zhang, L.-W. (2023b). Optimal reduced-order interval observer design for uncertain continuous-time linear systems. *International Journal of Robust and Nonlinear Control*, *33*(2), 1043–1064.
Lopez-Ramirez, F., Polyakov, A., Efimov, D., & Perruquetti, W. (2018). Finite-time and fixed-time observer design implicit Lyapunov function approach. *Automatica*, *87*, 52–60.
Luenberger, D. (1971). An introduction to observers. *IEEE Transactions on Automatic Control*, *16*(6), 596–602.
Ma, X., Huang, J., & Chen, L. (2019). Finite-time interval observers' design for switched systems. *Circuits, Systems, and Signal Processing*, *38*(11), 5304–5322.
Mazenc, F., Malisoff, M., & Niculescu, S.-I. (2022). Sampled-data estimator for nonlinear systems with uncertainties and arbitrarily fast rate of convergence. *Automatica*, *142*, Article 110361.
Meslem, N., Martinez, J., Ramdani, N., & Besançon, G. (2020). An interval observer for uncertain continuous-time linear systems. *International Journal of Robust and Nonlinear Control*, *30*(5), 1886–1902.
Meslem, N., & Ramdani, N. (2020). A new approach to design set-membership state estimators for discrete-time linear systems based on the observability matrix. *International Journal of Control*, *93*(11), 2541–2550.
Schweppe, F. (1968). Recursive state estimation: Unknown but bounded errors and system inputs. *IEEE Transactions on Automatic Control*, *13*(1), 22–28.
Sun, F., Huang, J., Ma, X., & Wen, X. (2020). Finite-time interval observer design for discrete-time switched systems: A linear programming approach. *Measurement and Control*, *53*(7–8), 1388–1394.
Tang, W., Wang, Z., Wang, Y., Raïssi, T., & Shen, Y. (2019). Interval estimation methods for discrete-time linear time-invariant systems. *IEEE Transactions on Automatic Control*, *64*(11), 4717–4724.
Wang, Z., Dinh, T. N., Zhang, Q., Raissi, T., & Shen, Y. (2022a). Fast interval estimation for discrete-time linear systems: An l1 optimization method. *Automatica*, *137*, Article 110029.
Wang, Z., Ma, Y., Zhang, Q., Tang, W., & Shen, Y. (2024). Interval estimation for time-varying descriptor systems via simultaneous optimizations of multiple interval widths. *IEEE Transactions on Systems, Man, and Cybernetics: Systems*, *54*(6), 3774–3782.
Wang, Z., Yin, H., Dinh, T. N., & Raïssi, T. (2022b). Interval estimation based on the reduced-order observer and peak-to-peak analysis. *International Journal of Control*, *95*(10), 2876–2884.
Wang, Z., Zhang, Y., Shen, M., & Shen, Y. (2022c). Ellipsoidal set-membership filtering for discrete-time linear time-varying systems. *IEEE Transactions on Automatic Control*, *68*(9), 5767–5774.
Xu, F. (2021). Generalized set-theoretic interval observer using element-wise nonnegativity transformation. *Automatica*, *125*, Article 109452.
Xu, F., Yang, S., & Liang, B. (2020a). Interval set-membership estimation for continuous linear systems. *International Journal of Robust and Nonlinear Control*, *30*(14), 5305–5321.
Xu, F., Yang, S., & Wang, X. (2020b). A novel set-theoretic interval observer for discrete linear time-invariant systems. *IEEE Transactions on Automatic Control*, *66*(2), 773–780.
Zhang, J., Chadli, M., & Wang, Y. (2019). A fixed-time observer for discrete-time singular systems with unknown inputs. *Applied Mathematics and Computation*, *363*, Article 124586.
Zhang, J., Song, Y., & Zheng, G. (2025). Prescribed-time observer for descriptor systems with unknown input. *Automatica*, *172*, Article 111999.
Zhou, M., Li, H., Xue, T., Wang, J., & Raïssi, T. (2025). Event-triggered state interval estimation and fault-tolerant control for multi-agent systems under deception attacks. *IEEE Transactions on Automatic Control*, *70*(1), 689–696.
Zhu, F., & Li, M. (2024). Distributed interval observer and distributed unknown input observer designs. *IEEE Transactions on Automatic Control*, *69*(12), 8868–8875.

Longwen Liu received his MS degree in the School of Automation Engineering from Northeast Electric Power University, Jilin, China, in 2019 and his Ph.D. degree in the College of Automation Science and Technology, South China University of Technology, Guangzhou, China, in 2023. He is currently a lecturer with School of Automation and Electronic Information, Xiangtan University, Hunan, China. His research interests include interval observer design, applications of positive systems, parametric method, and descriptor system.

Thach Ngoc Dinh received the Engineering and M.Sc.Res. degrees in Electrical Engineering and Automatic Control from INSA Lyon, France, in 2011, the Ph.D. degree in Physics from Paris-Saclay University, France, in 2014, and the Accreditation to Supervise Research (HDR) in Automatic Control and Robotics from Cnam, France, in 2025. Since 2017, he has been an Associate Professor at Cnam, France. His research interests include observer design, robust control, and nonlinear systems, with applications to autonomous and energy systems. He serves as an Associate Editor for IEEE Control Systems Letters and The Journal of the Franklin Institute and as an Editor for Nonlinear Dynamics. He is a member of the IEEE CSS Technical Committee on Robust and Complex Systems and the IFAC Technical Committee on Linear Control Systems.